Structures of the superconducting oxides $Tl_2Ba_2CuO_6$ and $Bi_2Sr_2CuO_6$

C. C. Torardi, M. A. Subramanian, J. C. Calabrese, J. Gopalakrishnan, E. M. McCarron, K. J. Morrissey, T. R. Askew, R. B. Flippen, U. Chowdhry, and A. W. Sleight
Central Research and Development Department, E. I. du Pont de Nemours and Company, Experimental Station, Wilmington, Delaware 19898
(Received 30 March 1988)

The structures of $Tl_2Ba_2CuO_6$ and $Bi_2Sr_2CuO_6$ have been solved and refined from single-crystal x-ray diffraction data. The structures are essentially the same and have single Cu-O sheets separated by either Tl-O or Bi-O double layers. The $Tl_2Ba_2CuO_6$ structure is tetragonal with $a=3.87$ Å and $c=23.24$ Å, and there are strictly flat Cu-O sheets. $Bi_2Sr_2CuO_6$ has a lower-symmetry structure which may be approximated with an orthorhombic cell with $a=5.36$ Å, $b=5.37$ Å, and $c=24.62$ Å; however, this ignores superstructure reflections along both the a and c axes. The Tl-O layers are much more strongly bound to each other than are the Bi-O layers; thus, better conduction along the c axis is expected for $Tl_2Ba_2CuO_6$ relative to $Bi_2Sr_2CuO_6$. Superconducting transition temperatures of 9 and 90 K were observed for $Bi_2Sr_2CuO_6$ and $Tl_2Ba_2CuO_6$, respectively.

Recent announcements of superconductivity at onset temperatures above 100 K in the new class of Bi-Sr-Ca-Cu-O (Refs. 1 and 2) and Tl-Ba-Ca-Cu-O (Ref. 3) ceramics have prompted a flurry of activity aimed at the identification and structural characterization of the superconducting phases in these systems. Reports of T_c ranging from 7 to 22 K in the Bi-Sr-Cu-O system[4] contrast with observations of T_c close to 90 K in the structurally analogous Tl-Ba-Cu-O system.[5] To understand this intriguing effect of subtle structural changes in these copper-based oxides on T_c, we have grown single crystals of superconducting phases in these systems. It is now apparent that there is a series of superconducting phases which may be represented as $(A^{III}O)_2A_2^{II}Ca_{n-1}Cu_nO_{2+2n}$ where A^{III} is Bi or Tl, A^{II} is Sr or Ba, and n is the number of consecutive Cu-O layers. Here we report on the identification and structural characterization of powders and crystals of the $n=1$ phases in the Bi and Tl systems. The $Tl_2Ba_2CuO_6$ phase represents the first example of superconductivity in the copper-oxide-based material with strictly planar Cu-O sheets.

Powder samples in the Tl-Ba-Cu-O and Bi-Sr-Cu-O systems were prepared by heating at 850–950 °C for 1–6 h mixtures of high-purity oxides (BaO_2, Tl_2O_3, and CuO; Bi_2O_3, SrO_2, and CuO, respectively) in sealed gold tubes for Tl (Ba) composition and open gold crucibles for Bi (Sr) composition. In the case of Tl (Ba) composition, reaction of a 2:2:1 (Tl:Ba:Cu) mixture at 850 °C in air resulted in a superconducting phase with a characteristic x-ray reflection at a d spacing at 11.5 Å. Flux-exclusion measurements on this sample showed a T_c onset of 55 K. When the same mixture was heated to 875 °C, the x-ray data again indicated the presence of the 11.5-Å line, along with trace amounts of $BaCuO_2$. This material showed a T_c onset of 84 K and apparent zero resistivity at 79 K. On heating to 900 °C, the 2:2:1 (Tl:Ba:Cu) mixture partially melted and the x-ray pattern showed large amounts of $BaCuO_2$ along with the superconducting phase and traces of Tl_2O_3. Flux-exclusion measurements (Fig. 1) on this product indicated a T_c onset of ~90 K and electrical measurements showed apparent zero resistivity at 83 K

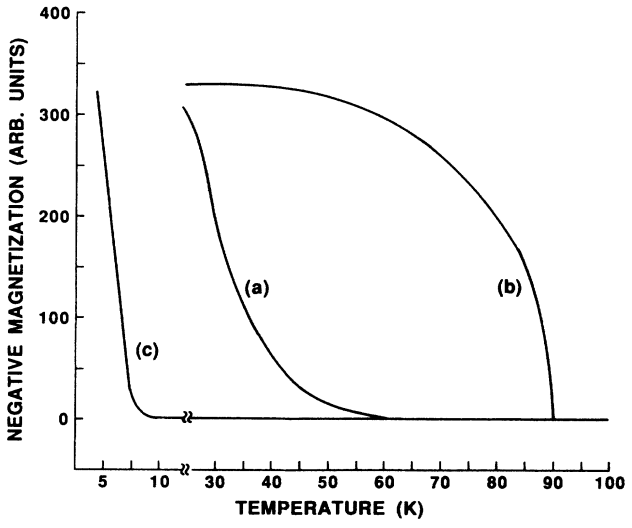

FIG. 1. Flux exclusion data: (a) $Tl_2Ba_2CuO_6$ prepared at 850 °C, (b) $Tl_2Ba_2CuO_6$ prepared at 900 °C, (c) $Bi_2Sr_2CuO_6$.

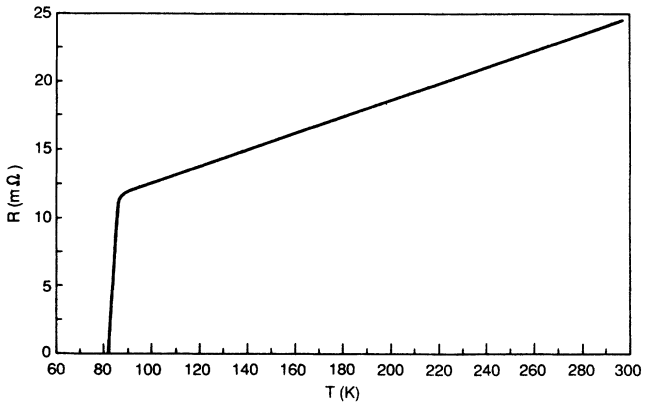

FIG. 2. Resistivity data for $Tl_2Ba_2CuO_6$ prepared at 900 °C.

(Fig. 2). We have observed a similar dependence of T_c on synthesis conditions in the Bi-Sr-Cu-O system but have not yet studied this in detail. Therefore, within each system, even though the x-ray patterns of the superconducting phases appear to be similar, the T_c of the material is strongly dependent on the thermal history of the sample. It is likely that some intergrowth occurs in the large unit cells of these materials. Examination of the x-ray powder data for $Tl_2Ba_2CuO_6$ indicated a tetragonal unit cell with $a=3.86$ Å and $c=23.2$ Å. Likewise, the powder pattern of $Bi_2Sr_2CuO_6$ could be indexed on the basis of a tetragonal cell with $a=5.37$ Å and $c=24.6$ Å. However, the presence of weak impurity lines complicates the indexing of the patterns. A preliminary structure for $Bi_2Sr_2CuO_6$ based on powder x-ray diffraction data has recently been proposed.[6]

Single crystals of $Tl_2Ba_2CuO_6$ were synthesized in sealed gold tubes by heating the reactants in the molar ratio 2:2:2 (Tl:Ba:Cu) to provide a copper-rich melt. Upon slow cooling, black crystals were seen embedded in a multiphase mix. Flux-exclusion measurements on these black platelike crystals showed a T_c onset at about 90 K. Electrical transport measurements indicated apparent zero resistivity at 83 K. Similarly, single crystals of superconducting $Bi_2Sr_2CuO_6$ were grown from an off-stoichiometric 2:3:3 (Bi:Sr:Cu) mixture. Flux-exclusion measurements made on the black micaceous flakes revealed a T_c slightly above 9 K (Fig. 1).

The morphologies of the $Tl_2Ba_2CuO_6$ and $Bi_2Sr_2CuO_6$ crystals are shown in Figs. 3(a) and 3(b). The micalike nature of the $Bi_2Sr_2CuO_6$ flakes can be contrasted with the platy $Tl_2Ba_2CuO_6$ crystals which exhibit a lesser tendency to delaminate. Electron diffraction studies were conducted on these crystals using a Philips CM12 transmission electron microscope. These investigations show that $Bi_2Sr_2CuO_6$ has orthorhombic symmetry with $a=5.37$ Å, $b=5.36$ Å, $c=24.60$ Å with some monoclinic distortion (Fig. 4). Like the $Bi_2Sr_2CaCu_2O_8$ system,[7-9]

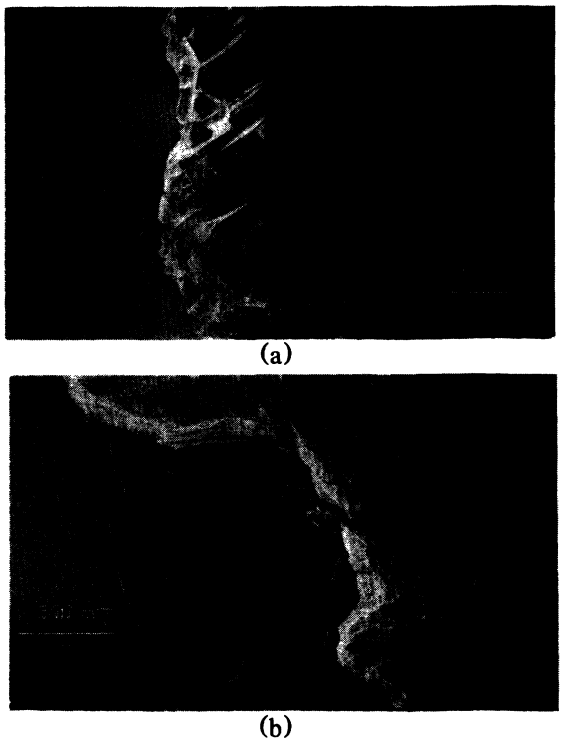

FIG. 3. Scanning electron micrographs of crystals of (a) $Tl_2Ba_2CuO_6$ and (b) $Bi_2Sr_2CuO_6$.

there is a superstructure along the a axis in $Bi_2Sr_2CuO_6$ as well. A 90° misorientation about [001] between layers can mistakenly lead to the conclusion that the superstructure is along both a and b axes. A threefold modulation along c has also been observed. The $Tl_2Ba_2CuO_6$ crystals show tetragonal symmetry with $a=3.86$ Å, $c=23.2$ Å as obtained from convergent-beam electron diffraction (Fig. 5). No superstructure was observed in this system. The crystals are essentially twin free but do show some dislo-

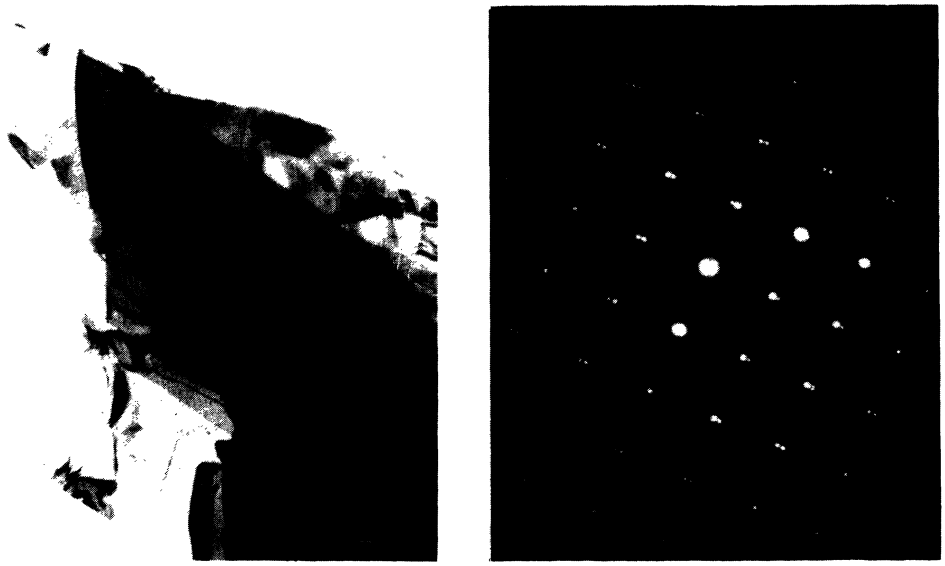

FIG. 4. Bright-field image (left) and selected-area diffraction pattern (right) from the basal plane of $Bi_2Sr_2CuO_6$.

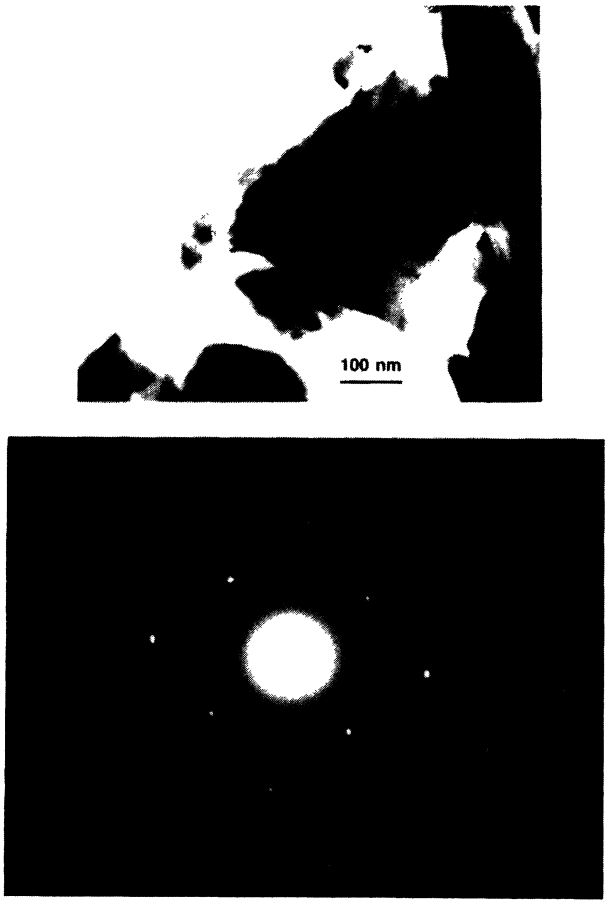

FIG. 5. Bright-field image (top) and selected-area diffraction pattern (bottom) of the basal plane of $Tl_2Ba_2CuO_6$.

cations. When these specimens were cooled in the microscope using a liquid-nitrogen stage, no change in symmetry was apparent in convergent-beam electron diffraction. The symmetry appears to stay tetragonal through the superconducting transition with no appearance of a superstructure.

Room-temperature single-crystal x-ray diffraction information for $Tl_2Ba_2CuO_6$ and $Bi_2Sr_2CuO_6$ is summarized in Table I. A black, plate-shaped crystal of $Tl_2Ba_2CuO_6$ was indexed as tetragonal with cell constants of $a=3.87$ and $c=23.24$ Å. The cell was transformed by $a\sqrt{2}$ to give $a=5.47$ Å in order to allow for the presence of supercell reflections and lower symmetry distortions as observed for $Bi_2Sr_{3-x}Ca_xCu_2O_8$.[7] Unlike the Bi material, the Tl crystals did not display the a-axis satellite modulation, and, in this respect, were similar to the crystals of $Tl_2Ba_2CaCu_2O_8$.[10,11] Examination of the data clearly showed the absence of F-centered violations, and the cell was subsequently transformed to the body-centered 3.866×23.239 Å tetragonal cell. The data were reduced to structure factors in the usual fashion, corrected for absorption, transformed, and averaged in $I4/mmm$ symmetry. Heavy-atom positions were located by direct methods,[12] and the oxygen atom positions were determined by difference Fourier synthesis. Refinement of the structure was achieved by full-matrix least-squares analysis using neutral-atom scattering-factor curves with anomalous scattering terms for the metal atoms, a term for isotropic secondary extinction, and anisotropic thermal motion for all atoms. Metal-atom sites were found to be fully occupied within two standard deviation units. The refinement indicated a high thermal dispersion for atom O(3) with $B_{11}=B_{22}=9(1)$ Å^2 as seen in the structure of

TABLE I. Summary of crystallographic information for $Tl_2Ba_2CuO_6$ and $Bi_2Sr_2CuO_6$.

	$Tl_2Ba_2CuO_6$	$Bi_2Sr_2CuO_6$
Dimensions (mm)	0.08×0.08×0.02	0.37×0.17×0.01
Diffractometer	CAD4	CAD4
Radiation	Mo $K\alpha$	Mo $K\alpha$
Monochromator	Graphite	Graphite
Formula weight	842.9	752.7
Crystal system	Tetragonal	Orthorhombic
Space group	$I4/mmm$ (No. 139)	$Amaa$ (No. 66)
Cell constants (Å) a	3.866(1)	5.362(3)
Cell constants (Å) b	. . .	5.374(1)
Cell constants (Å) c	23.239(6)	24.622(6)
Temperature	Ambient	Ambient
Calc. density (g cm^{-3})	8.07	7.03
Scan mode	ω	ω
2θ range (deg)	0–60	0–55
Octants	+++, −++	+++
μ (cm^{-1})	609.6	668.2
Absorption correction	Analytical	Analytical
Transmission factors	0.026–0.230	0.017–0.453
Extinction parameter (mm)	$4.3(4)\times10^{-5}$	. . .
Total reflections	2302	1605
Independent reflections ($I\geq3\sigma$)	164	235
Data per parameter	8.2	9.4
R	0.021	0.130
R_w	0.022	0.130

TABLE II. Positional [space group *I4/mmm* (No. 139)] and thermal parameters for the atoms of $Tl_2Ba_2CuO_6$. All atoms except O(3) refined with anisotropic thermal parameters; the equivalent isotropic thermal parameter is listed.

Atom	Site	x	y	z	B (Å^2)
Tl(1)	4*e*	0.50	0.50	0.20265(2)	1.3(1)
Ba(1)	4*e*	0.00	0.00	0.08301(3)	0.5(1)
Cu(1)	2*b*	0.50	0.50	0.00	0.4(1)
O(1)	4*c*	0.00	0.50	0.00	0.7(1)
O(2)	4*e*	0.50	0.50	0.1168(4)	1.1(1)
O(3)	16*n*	0.595(5)	0.50	0.2889(5)	0.4(3)

$Tl_2Ba_2CaCu_2O_8$.[11] Refining this oxygen atom off its ideal 4*mm* sites results in a 0.4-Å displacement, a lower isotropic thermal parameter (B=0.4 Å^2), and a locally distorted thallium environment. The largest peak in a final difference Fourier was 0.1 e/Å^3 located 1.0 Å from O(1).

Due to the micaceous nature of the material, frequent stacking faults and imperfections occurred in crystals of $Bi_2Sr_2CuO_6$. Precession and axial oscillation photographs, as well as electron diffraction patterns, showed the presence of satellite reflections as seen for $Bi_2Sr_{3-x}Ca_x$-Cu_2O_8.[7,8] Unfortunately, the satellites were always observed along both the *a* and *b* axes indicating a twinning or 90° misorientation problem. Analogous to the superstructure observed in the Bi-Sr-Ca-Cu material, the satellite reflections in $Bi_2Sr_2CuO_6$ suggest a supercell where the *a* axis is approximately a factor of 5 times the subcell dimension. The crystals are further complicated by a modulation along the *c* axis with a periodicity of approximately 3 times the 24.6-Å *c* dimension. A crystal that showed satellite reflections more strongly along one of the basal axes (assigned as the *a* axis) was selected. Data were collected on a "subcell" that was indexed as orthorhombic (pseudotetragonal) with a=5.36, b=5.37, and c=24.62 Å. Evidence for the ~5.4-Å cell edges was found in precession photographs, electron diffraction patterns, and convergent beam electron diffraction experiments. Weak violations for *A* centering were present in the observed data, but these reflections were not included in the structural refinement. The remaining data were compatible with the space group *Amaa*. Metal-atom positions were located from a Patterson map and oxygen atoms were found in electron difference maps. Full-matrix least-squares refinement included anomalous scattering terms and anisotropic thermal motion for the metal atoms. Within 1–2 standard deviation units, metal-atom sites were found to be fully occupied. Large anisotropic B_{11} and B_{33} thermal parameters (Table V) for the metal atoms are consistent with the *a*- and *c*-axis satellite reflections and are probably due to "subcell disorder" (long-range order) of the bismuth-oxygen layers. The two independent oxygen atoms, O(2) and O(3), that are associated with the bismuth atoms display large isotropic motion, also consistent with the observed bismuth-layer situation. The highest peak in a final difference Fourier map was 2.9 e/Å^3, 0.9 Å from Sr. Data were collected on a second crystal of $Bi_2Sr_2CuO_6$ with a=5.361(2), b=5.370(1), c=24.369(6) Å that was grown from a Bi-Sr-Ca-Cu-O mixture. The structural refinement (173 independent reflections, $R\sim R_w\sim 0.10$, *Amaa*, data to parameter ratio 6.0) yielded essentially identical atomic positions and thermal parameters.

Positional and thermal parameters for $Tl_2Ba_2CuO_6$ are given in Tables II and III, and those for $Bi_2Sr_2CuO_6$ are given in Tables IV and V. Interatomic distances for both compounds are listed in Table VI.

The crystal structures of $Tl_2Ba_2CuO_6$ and $Bi_2Sr_2CuO_6$ are almost identical to one another and are related to the recently reported structures of $Tl_2Ba_2CaCu_2O_8$ (Ref. 11) and $Bi_2Sr_{3-x}Ca_xCu_2O_8$.[7–9] The 2:2:1 compounds possess single sheets of corner-sharing CuO_4 units in which each copper atom has two additional oxygen atoms positioned above and below the sheet to form an axially elongated (Jahn-Teller-distorted) octahedron. The 2:2:1:2 phases contain double sheets of corner-sharing CuO_4 moieties separated by calcium ions, and have each copper atom associated with a fifth oxygen atom at distances of ~2.5–2.7 Å, forming a square pyramid around copper. All four compounds have Ba or Sr ions located just above and below the single or double sheets. These alkaline-earth copper-oxide slabs alternate with double Bi-O or Tl-O sheets and are stacked along the *c* axis (Fig. 6).

TABLE III. Anisotropic thermal parameters (Å^2) for the atoms of $Tl_2Ba_2CuO_6$. Parameters are given by the expression $\exp\{-0.25[B_{11}h^2a^{*2}\cdots+2(B_{12}hka^*b^*\cdots)]\}$.

Atom	B_{11}	B_{22}	B_{33}	B_{12}	B_{13}	B_{23}
Tl(1)	1.71(3)	1.71	0.52(2)	0.00	0.00	0.00
Ba(1)	0.49(3)	0.49	0.65(3)	0.00	0.00	0.00
Cu(1)	0.2(1)	0.2	0.8(1)	0.00	0.00	0.00
O(1)	0.5(4)	0.7(4)	0.8(2)	0.0	0.0	0.0
O(2)	1.6(3)	1.6	0.3(2)	0.0	0.0	0.0

TABLE IV. Positional [space group *Amaa* (No. 66, nonconventional setting of *Cccm*): (0,0,0; $0,\frac{1}{2},\frac{1}{2}$)$(x,y,z;\ -x,y,z;\ \frac{1}{2}+x,-y,z;\ \frac{1}{2}+x,y,-z)$] and thermal parameters for the atoms of $Bi_2Sr_2CuO_6$. Metal atoms refined with anisotropic thermal parameters; equivalent isotropic thermal parameter is listed.

Atom	Site	x	y	z	B (Å^2)
Bi(1)	8*l*	0.00	0.2758(5)	0.0660(2)	5.9(1)
Sr(1)	8*l*	0.50	0.2479(9)	0.1790(4)	2.8(2)
Cu(1)	4*e*	0.50	0.75	0.25	4.3(5)
O(1)	8*g*	0.75	0.50	0.246(2)	0.5(6)
O(2)	8*l*	0.00	0.226(12)	0.145(4)	8.6(26)
O(3)	8*l*	0.50	0.334(15)	0.064(5)	9.3(25)

In the single copper-oxygen sheets of $Tl_2Ba_2CuO_6$, the Cu−O bond distances are 1.933 Å. These are longer than the corresponding bonds in $Bi_2Sr_2CuO_6$, 1.900 Å. The additional oxygen atoms located above and below the sheets are positioned at a distance of 2.71 Å (Tl) and 2.6 Å (Bi) from the copper atoms. The distorted octahedra in $Tl_2Ba_2CuO_6$ have D_{4h} (4/*mmm*) site symmetry and have copper with its four equatorial O atoms lying on a mirror plane. However, the octahedra in the Cu-O sheets of $Bi_2Sr_2CuO_6$ have approximately C_{2v} (2/*m*) site symmetry and are alternately tilted in the (100) planes. This same arrangement of corner-shared octahedra is also found in the single Cu-O sheets of La_2CuO_4 (Ref. 13) in which the Cu-O distances are 1.91 Å (equatorial) and 2.46 Å (apical). The tilted octahedra in La_2CuO_4 appear to be responsible for its distortion from the tetragonal K_2NiF_4-type structure, $a=3.81$ Å and $c=13.2$ Å, to the observed room-temperature orthorhombic structure, $a=5.41$, $b=5.37$, $c=13.2$ Å. The Cu−O−Cu bond angle in the Cu-O sheets is 180° when the octahedra are not tilted, but deviates from this angle as the octahedra are tilted. This angle is expected to be linear for longer Cu-O distances as in $Tl_2Ba_2CuO_6$ and the R_2CuO_4 phases where R is Pr, Nd, Sm, or Gd.[14] However, the tendency for Cu−O−Cu bond bending, and thus octahedra tilting, increases as the Cu-O distance decreases. All previously known copper oxide superconductors had bent Cu−O−Cu bonds; thus, the Cu-O sheets were not strictly planar. The $Tl_2Ba_2CuO_6$ phase represents the first example of superconductivity in a copper-oxide-based material where the Cu-O sheets are strictly planar.

Barium ions reside just above and below the Cu-O single sheets of $Tl_2Ba_2CuO_6$ in nine coordination with oxygen. The Ba-Cu-Ba layers alternate with a double thallium-oxygen layer giving a layer repeat sequence of ··· Tl-Tl-Ba-Cu-Ba ··· along the c direction. Thallium bonds to six oxygen atoms in a distorted octahedral arrangement. The Tl-O double layers are essentially identical to those found in $Tl_2Ba_2CaCu_2O_8$ (Ref. 11) and are composed of edge-sharing TlO_6 octahedra. The size of the a axis tends to be determined by the Cu−O bonds in the Cu-O sheets, and the spacing of the Tl and O in the a-b plane is constrained by symmetry to give Tl-O distances of 2.73 Å if Tl and O(3) have the same z parameter. This Tl-O distance of 2.73 Å is much larger than the 2.29-Å value calculated from the sum of Tl^{III} and O^{II-} radii.[15] Some compensation of these long distances occurs through short Tl-O distances of 2.00 and 2.04 Å along the c axis. As observed in $Tl_2Ba_2CaCuO_8$,[11] the oxygen atom situated in the Tl-O layers, O(3), shows highly anisotropic dispersion when refined on the 4*e* site $(\frac{1}{2},\frac{1}{2},z)$. With O(3) statistically distributed on the 16*n* sites, the locally distorted Tl environment then contains two short and two long intrasheet Tl-O distances of 2.50 and 3.01 Å.

A similar structural arrangement exists for $Bi_2Sr_2CuO_6$ with regard to the metal-atom layers, but, because of apparent disorder in the subcell, the precise nature of the bismuth-oxygen bonding is not yet understood. The same situation is also observed in the double bismuth-oxygen layers of $Bi_2Sr_{3-x}Ca_xCu_2O_8$. Single-crystal and powder neutron-diffraction experiments are in progress with the goal of understanding the bismuth-oxygen atomic arrangement and bonding.

The nature of the Bi-O versus the Tl−O bonding within the double layers is likely to be responsible for the different morphologies of the two materials. The micalike character of $Bi_2Sr_2CuO_6$ and $Bi_2Sr_2CaCu_2O_8$ is presumably due to weak intersheet Bi−O bonds. In these materials, the distance between adjacent bismuth sheets is ~3.25 Å. Cleavage between the Bi-O layers yields charge neutral sections. The interaction between the neighboring Tl-O sheets in $Tl_2Ba_2CuO_6$ and $Tl_2Ba_2CaCu_2O_8$ is much stronger. Intersheet Tl−O bonds are ~2.0 Å in length and the separation between the two Tl

TABLE V. Anisotropic thermal parameters (Å^2) for the metal atoms of $Bi_2Sr_2CuO_6$. Parameters are given by the expression $\exp\{-0.25[B_{11}h^2a^{*2}\cdots+2(B_{12}hka^*b^*\cdots)]\}$.

Atom	B_{11}	B_{22}	B_{33}	B_{12}	B_{13}	B_{23}
Bi(1)	10.1(3)	1.5(1)	6.1(3)	0.4(1)	−5.1(1)	−0.5(1)
Sr(1)	0.7(2)	0.5(2)	7.2(6)	0.0	0.0	−0.2(3)
Cu(1)	1.7(5)	0.3(4)	11.0(15)	0.0	0.0	0.1(5)

TABLE VI. Interatomic distances (Å) in $Tl_2Ba_2CuO_6$ and $Bi_2Sr_2CuO_6$.

	$Ti_2Ba_2CuO_6$	$Bi_2Sr_2CuO_6$
Cu-O(1)	1.9330(5)(×4)	1.900(2)(×4)
Cu-O(2)	2.714(9) (×2)	2.58(11)(×2)
Tl(Bi)-O(2)	1.995(9) (×1)	1.97(11)(×1)
Tl(Bi)-O(3)	2.038(11)(×1)	2.10(9) (×1)
Tl(Bi)-O(3)	2.496(12)(×2)	2.70(1) (×2)
Tl(Bi)-O(3)	3.011(15)(×2)	3.21(11)(×1)
		3.28(9) (×1)
Ba(Sr)-O(1)	2.7309(7)(×4)	2.53(3) (×2)
		2.64(3) (×2)
Ba(Sr)-O(2)	2.844(2) (×4)	2.95(7) (×1)
		2.81(3) (×2)
		2.68(7) (×1)
Ba(Sr)-O(3)	2.999(11)(×1)	2.87(11)(×1)

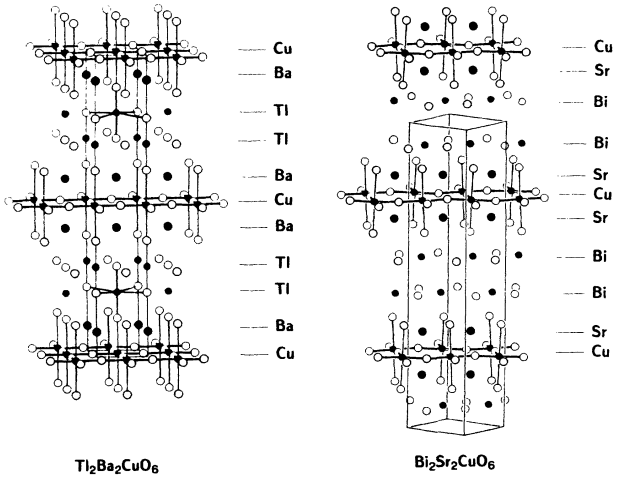

FIG. 6. Structure of $Tl_2Ba_2CuO_6$ and $Bi_2Sr_2CuO_6$. Metal atoms are shaded and Cu−O bonds are shown.

layers is 2.2 Å, which makes the crystals brittle and more difficult to cleave. The difference in the intersheet bonding of the Tl-O and Bi-O double layers is reflected in the *c*-axis length of the two compounds. Although the average ionic radii[15] of Tl (Ba) (1.18 Å) and Bi (Sr) (1.17 Å) are almost identical, the *c* axis for the bismuth phase is 1.4 Å longer than that of the thallium material.

The structures of both $Tl_2Ba_2CuO_6$ and $Tl_2Ba_2CaCu_2O_8$ are tetragonal by diffraction measurements that actually determine the average symmetry of many unit cells. However, the disorder of the oxygens in the Tl-O double layers indicates that the local symmetry is lower than tetragonal. A similar situation exists for certain $La_{1+x}Ba_{2-x}Cu_3O_{7+y}$ superconductors.[16] Thus a common feature of all copper-oxide-based superconductors is tetragonal pseudosymmetry which is always, at least locally, reduced.

Speculation with regard to structure-property relations is difficult for $Bi_2Sr_2CuO_6$ and $Bi_2Sr_2CaCu_2O_8$ because of uncertainties in details of their structure and composition. Even $Tl_2Ba_2CaCu_2O_8$ is complicated by apparent mixing of Tl and Ca on each other's sites.[11] The structure and composition of $Tl_2Ba_2CuO_6$ are well defined and the simplest representation of oxidation states would be $(Tl_2^{III}Ba_2^{II}Cu^{II}O_6^{II-})$. However, there is almost certainly significant mixing of Cu^{3d} and Tl^{6s} states with the likely result that some trivalent copper is created, i.e., $Tl_{2-x}^{III}Tl_x^{II}Ba_2^{II}Cu_{2-x}^{II}Cu_x^{III}O_6$. In fact, there is precedent for this behavior of Tl in $Tl_2^{III}Ru_2^{IV}O_7$ where it has been shown[17] that Tl^{III} has oxidized at least some Ru^{IV} to Ru^{V}. The partial reduction of Tl^{III} to Tl^{II} in $Tl_2Ba_2CuO_6$ may be enhanced by the fact that the Tl site is actually somewhat too large for Tl^{III}. Thus the presence of mixed Cu^{II}-Cu^{III} is very likely in $Tl_2Ba_2CuO_6$, and this mixed valency then apparently remains a common characteristic of all copper-oxide-based superconductors. It would appear that the primary difference between the Tl and Bi phases is that the Tl phases are much more tightly coupled, structurally and electronically, along the *c* axis. This better coupling in the Tl phases may in turn relate to the higher T_c's for these materials.

We gratefully acknowledge the following colleagues for their assistance with this publication: P. M. Kelly, C. R. Walther, R. A. Oswald, W. J. Marshall, L. F. Lardear, D. L. Smith, D. M. Groski, L. Cooke, C. M. Foris, A. J. Pawlowski, G. M. Hyatt, and N. Budynkiewicz.

[1]H. Maeda, Y. Tanaka, M. Fukutomi, and T. Asano, Jpn. J. Appl. Phys. **27**, L209 (1988).

[2]C. W. Chu, J. Bechtold, L. Gao, P. H. Hor, Z. J. Huang, R. L. Meng, Y. Y. Sun, Y. Q. Wang, and Y. Y. Xwe, Phys. Rev. Lett. **60**, 941 (1988).

[3]Z. Z. Sheng and A. M. Hermann, Nature **332**, 138 (1988).

[4]C. Michel, M. Hervieu, M. M. Borel, A. Grandin, F. Deslandes, J. Provost, and B. Raveau, Z. Phys. B **68**, 421 (1987).

[5]Z. Z. Sheng and A. M. Hermann, Nature **332**, 55 (1988).

[6]J. B. Torrance, Y. Tokura, S. J. LaPlaca, T. C. Huang, R. J. Savoy, and A. I. Nazzal, Solid State Commun. **66**, 703 (1988).

[7]M. A. Subramanian, C. C. Torardi, J. C. Calabrese, J. Gopalakrishnan, K. J. Morrissey, T. R. Askew, R. B. Flippen, U. Chowdhry, and A. W. Sleight, Science **239**, 1015 (1988).

[8]S. A. Sunshine, T. Siegrist, L. F. Schneemeyer, D. W. Murphy, R. J. Cava, B. Batlogg, R. B. van Dover, R. M. Fleming, S. H. Glarum, S. Nakahara, R. Farrow, J. J. Krajewski, S. M. Zahurak, J. V. Waszczak, J. H. Marshall, P. Marsh, L. W. Rupp, Jr., and W. F. Peck, this issue, Phys. Rev. B **38**, 893 (1988).

[9]J. M. Tarascon, Y. LePage, P. Barboux, B. G. Bagley, L. H. Greene, W. R. McKinnon, G. W. Hull, M. Giroud, and D. M. Hwang, Phys. Rev. B **37**, 9382 (1988).

[10]R. M. Hazen, L. W. Finger, R. J. Angel, C. T. Prewitt, N. L. Ross, C. G. Hadidiacos, P. J. Heaney, D. R. Veblen, Z. Z. Sheng, A. El Ali, and A. M. Hermann, Phys. Rev. Lett. **60**, 1657 (1988).

[11]M. A. Subramanian, J. C. Calabrese, C. C. Torardi, J. Gopalakrishnan, T. R. Askew, R. B. Flippen, K. J. Morrissey, U. Chowdhry, and A. W. Sleight, Nature **332**, 420 (1988).

[12]The computer program MULTAN was used to solve the crystal structure. See P. Main *et al.*, MULTAN (Department of Physics, University of York, England, 1980).

[13]B. Grande, H. Müller-Buschbaum, and M. Schweizer, Z. Anorg. Allg. Chem. **428**, 120 (1977).

[14]A. W. Sleight, in *Chemistry of High-Temperature Superconductors,* edited by D. L. Nelson, M. S. Whittingham, and T. F. George, ACS Symp. Series No. 351 (American Chemical Society, Washington, DC, 1987), pp. 2–12.

[15]R. D. Shannon, Acta Crystallogr. Sect. A **32**, 751 (1976).

[16]E. M. McCarron, C. C. Torardi, J. P. Attfield, K. J. Morrissey, A. W. Sleight, D. E. Cox, R. K. Bordia, W. E. Farneth, R. B. Flippen, M. A. Subramanian, E. Lopdrup, and A. J. Poon, in *Proceedings of the Materials Research Society Symposium Boston, MA, 1987,* edited by M. B. Brodsky, R. C. Dynes, K. Kitazawa, and H. L. Tuller (MRS, Boston, 1988), Vol. 99, pp. 101–106.

[17]H. S. Jarrett, A. W. Sleight, J. F. Weiher, J. L. Gillson, C. G. Frederick, G. A. Jones, R. S. Swingle, D. Swartzfager, J. E. Gulley, and P. C. Hoell, in *Valence Instabilities and Related Narrow-Band Phenomenon,* edited by R. D. Parks (Plenum, New York, 1977), pp. 545–549.

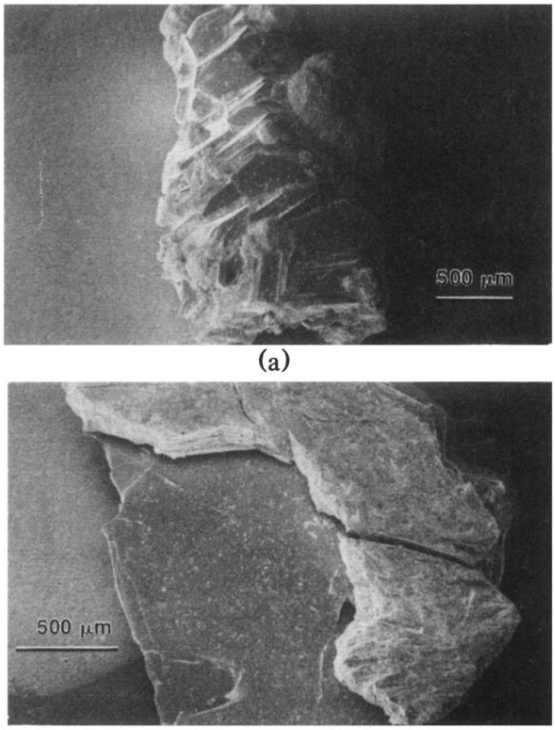

FIG. 3. Scanning electron micrographs of crystals of (a) $Tl_2Ba_2CuO_6$ and (b) $Bi_2Sr_2CuO_6$.

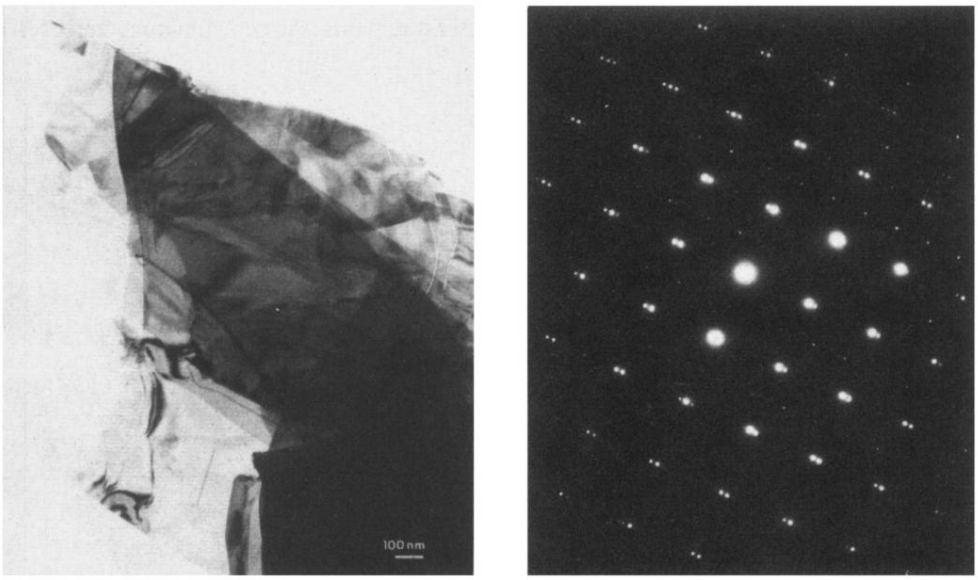

FIG. 4. Bright-field image (left) and selected-area diffraction pattern (right) from the basal plane of $Bi_2Sr_2CuO_6$.

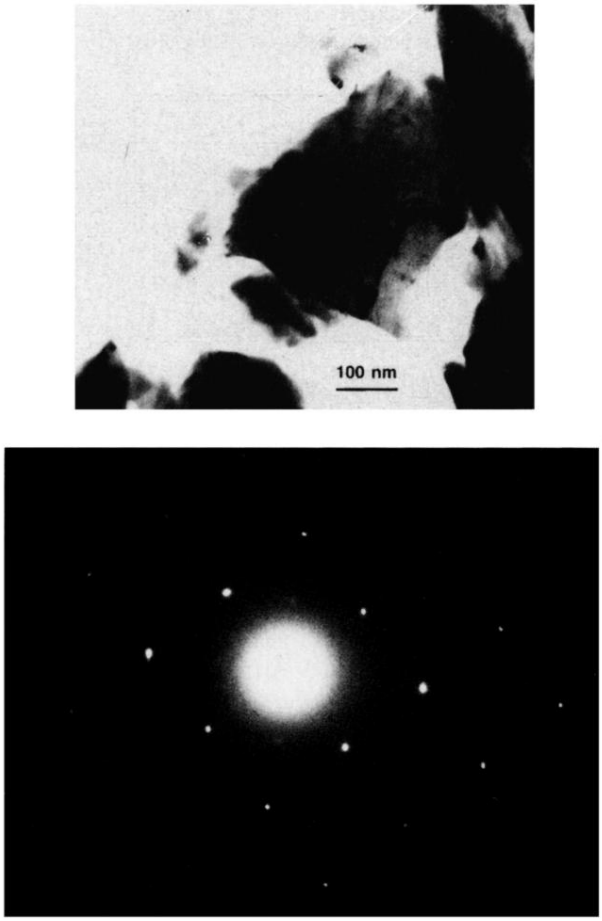

FIG. 5. Bright-field image (top) and selected-area diffraction pattern (bottom) of the basal plane of $Tl_2Ba_2CuO_6$.